Meteorol. Rdsch. 33, 14—18 (Februar 1980)

A comparison between global and one-dimensional energy balance models: Stability results

Th. Dümmel and H. Volkert

Berlin

Abstract. The stability of the equilibria of Sellers' [8] one dimensional climate model can simply be determined from the global net radiation imbalance. This is possible by using an analogy between the steady state one-dimensional and time-dependent zero-dimensional version of energy balance climate models. The following results are obtained: Two stable equilibria representing the "present day" and "ice-covered earth" conditions are separated by an unstable steady state solution which defines a boundary for initial situations to be attracted by the related stable equilibrium.

Ein Vergleich zwischen globalen und eindimensionalen Energiebilanz-Klimamodellen: Stabilitätsergebnisse

Zusammenfassung. Die Stabilität der Gleichgewichtslösungen von Sellers' eindimensionalem Klimamodell [8] läßt sich einfach aus der unausgeglichenen globalen Strahlungsbilanz bestimmen. Dies wird durch eine Analogie zwischen stationärer und zeitabhängiger Version eines Energiebilanz-Klimamodells ermöglicht. Man erhält folgende Ergebnisse: Zwei stabile Gleichgewichtszustände, die die heutigen Bedingungen und die einer völlig eisbedeckten Erde darstellen, werden von einer instabilen Lösung getrennt. Diese stellt eine Grenze für Anfangswerte dar, die von den jeweiligen stabilen Gleichgewichtslösungen angezogen werden.

1. Introduction

This note deals with the stability of the equilibria of Sellers' [8] climate model. It is the intention to show that global stability interpretations on this system can directly be inferred from the basic steady state model version without explicitly calculating the time dependence [5, 7] or applying complex stability analyses [6]. This is made possible by an analogy between the time-dependent zero-dimensional and the steady state one-dimensional version of energy balance models.

2. Analogy between steady state one-dimensional and time-dependent zero-dimensional energy balance models

The time-dependent version of the zonally averaged and vertically integrated (i.e. one-dimensional) equation of the heat balance of the earth-atmosphere system is given by:

$$a\,c\,\frac{\partial T}{\partial t}\cos\varphi = a\,R(\varphi, T)\cos\varphi + \frac{\partial}{\partial\varphi}F(\varphi, T)\cos\varphi \qquad (2.1)$$

with the latitude φ, the thermal inertia $c > 0$, the earth's radius a, the zonally averaged meridional temperature distribution T and two latitude and temperature dependent quantities: the net-radiation R (in Wm^{-2}) and the meridional transport of total energy F (in Wm^{-1}). For parameterizations of R and F see Appendix b.

Two types of nonlinear approximations for (2.1) will be discussed in the following:

a) The neglect of energy storage together with integration over $i = 1,\ldots, 18$ individual 10 °-latitude belts ([8], Eq. 2) yields a steady state and one-dimensional discretized model equation:

$$0 = R_i(T)\cdot A_i + F_{i+1}(T)\cdot l_{i+1} - F_i(T)\cdot l_i \qquad (2.2)$$

with boundary conditions

$$F_1\cdot l_1 = 0 \qquad (2.3)$$

$$F_{19}\cdot l_{19} = 0, \qquad (2.4)$$

where the area A_i weighted net radiation R_i of each belt is balanced by the meridional energy fluxes in ocean and atmosphere F_i, F_{i+1} (northward positive) through the adjacent lateral boundaries l_i, l_{i+1}. Meridional temperature distributions consistent with (2.2), (2.3), (2.4) are equilibrium solutions and denoted as T^j. For those temperature distributions which are only consistent with (2.2) and (2.3) (i.e. $F_{19}\,l_{19} \neq 0$) one obtains

$$-\mathrm{Res}\,(T) \equiv F_{19}\cdot l_{19} = \sum_{i=1}^{18} R_i(T)\,A_i \cong \cong \int_{-\pi/2}^{\pi/2} R\,(\varphi, T)\cos\varphi\,d\varphi \qquad (2.5)$$

0026–1211/80/0033–0014 $ 02.25

where the negative residue Res (T) equals the global net radiation imbalance (within the approximation of the meridional discretization in latitude belts).

b) The global integration with the assumption of latitude independent thermal inertia c results in the time-dependent zero-dimensional model equation

$$c\frac{\partial \overline{T}}{\partial t} = \int_{-\pi/2}^{\pi/2} R(\varphi, T)\cos\varphi \, d\varphi \qquad (2.6)$$

with the time-dependent global mean surface temperature

$$\overline{T}\,(t) = \int_{-\pi/2}^{\pi/2} T(\varphi, t)\cos\varphi \, d\varphi$$

In order to establish an analogy between the cases a) and b) it is necessary to realize that for equilibrium solutions T^j of (2.2) the energy fluxes vanish at the poles (2.3, 2.4); i.e. an equilibrium T^j is obtained, for Res (T) = 0 in (2.5) disappears. This residue Res(T) can be calculated in a unique way after parameterizing the radiation balance $R_i(T)$ and the meridional energy flux $F_i(T)$ as a nonlinear function of the zonally averaged surface temperature (for details see [2, 8]) and prescribing the starting temperature T_1 (for the area between 90N and 80N).

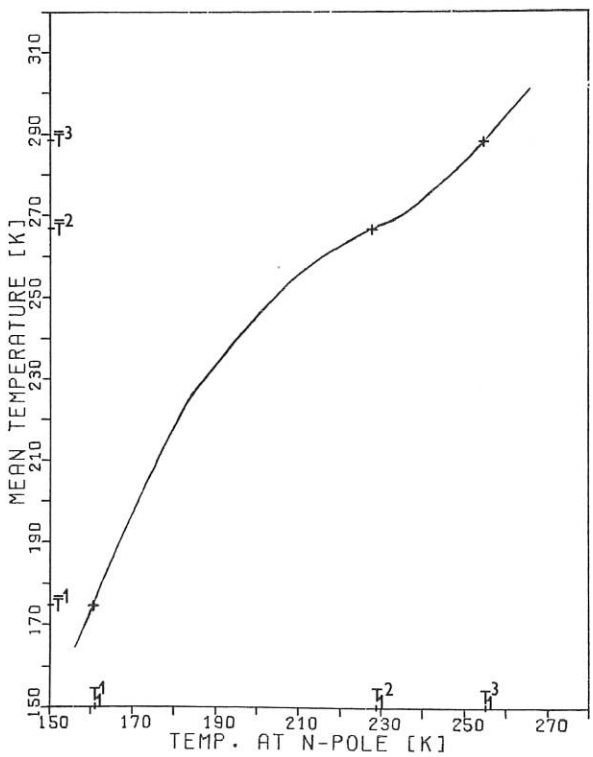

Fig. 1. Continuous monotone increasing relation between the starting temperature T^1 and global (mean surface) temperature $\overline{T}$. Upper indices denote the equilibrium solutions.

A bijective functional relationship (continuous monotone increasing) exists between the starting temperature T_1 and related global mean temperature $\overline{T}$ which is numerically established (Fig. 1). In the neighbourhood of the starting temperature $T^2{}_1$ increments of 0.005 K have been applied. Therefore, it is an obvious implication of the steady state one-dimensional model's iteration method that the global net radiation imbalance can be seen as a function of the global mean temperature alone, i.e. Res = Res($\overline{T}$). Thus, comparison of (2.5) and (2.6) reveals that the residue of a meridional temperature distribution T is directly proportional to the temperature tendency of the zero-dimensional representation of the model.

The next section will show how the stabilities of the equilibrium solutions in Sellers' climate model and their physical interpretation can be directly deduced using the above-mentioned analogy.

3. Stability results in Sellers' (1969) climate model and their physical interpretation

In Fig. 2 the function Res ($\overline{T}$) is plotted for three values of the relative intensity μ of the solar constant. For the "present day" value of the solar constant ($\mu = 1.00$) the model shows the three well-known [6] equilibrium solutions (Res = 0) with global mean temperatures $\overline{T}^1 = 175K$, $\overline{T}^2 = 267K$, $\overline{T}^3 = 288.5K$ and the related starting temperatures at the N-pole $T^1{}_1 = 161K$, $T^2{}_1 = 229K$, $T^3{}_1 = 255.5K$, respectively (see Fig. 1). $\overline{T}^1 = 175K$ characterizes an "ice-covered" earth. It is a globally stable equilibrium solution because the residua in its neighbourhood lead to temperature tendencies towards this situation, i.e. an initial temperature distribution with $\overline{T} \leqslant \overline{T}^1$ yields a residuum Res $\leqslant 0$ which is equivalent to $\partial\overline{T}/\partial t \geqslant 0$ (see section 2). $\overline{T}^3 = 288.5K$ represents the "present day" climate state which is another stable equilibrium because the neighbouring temperature tendencies are directed towards it ($\overline{T} \gtrless \overline{T}^3$ leads to Res $\gtrless 0$ and thus $\partial\overline{T}/\partial t \leqslant 0$). $\overline{T}^2 = 267K$, however, is an unstable equilibrium. Any residuum in its neighbourhood results in a global temperature tendency which is repelling the globally averaged state variable $\overline{T}$ from this situation. The subsequent direction of the globally averaged temperature flow tends (i) towards the "ice-covered" earth $\overline{T}^1$ for starting conditions which result in $\overline{T} < \overline{T}^2$, and (ii) towards the "present day" situation $\overline{T}^3$ for initial values equivalent to $\overline{T} > \overline{T}^2$ (as indicated by the arrows in Fig. 2, for $\mu = 1.00$). Thus, $\overline{T}^2$ represents a climate which cannot evolve from any initial conditions with a global mean temperature $\overline{T} \neq \overline{T}^2$. Therefore the unstable steady state $\overline{T}^2$ can hardly be interpreted as an "ice-age" climate (as done by Crafoord and Källén [1]; instead, $\overline{T}^2$ must be seen as the boundary for initial values $\overline{T}$ between the attractive basins of the stable equilibrium solutions $\overline{T}^1$ and $\overline{T}^3$, respectively.

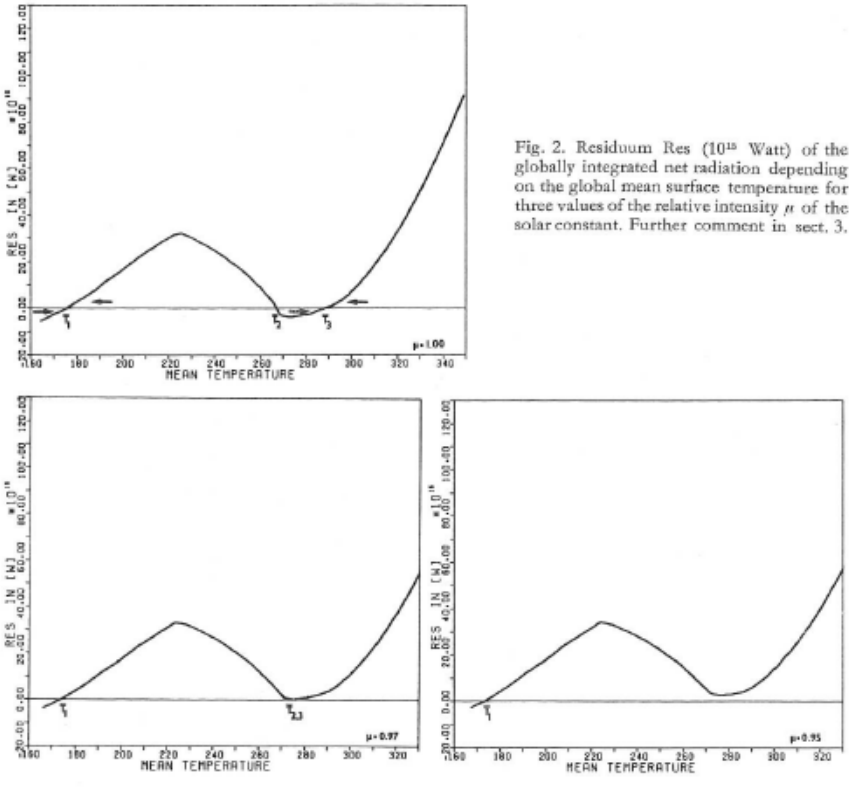

Fig. 2. Residuum Res (10^{15} Watt) of the globally integrated net radiation depending on the global mean surface temperature for three values of the relative intensity μ of the solar constant. Further comment in sect. 3.

The two other graphs of Fig. 2 can analogously be interpreted. They are distinguished from one another by the incoming solar radiation being gradually decreased by 3% ($\mu = 0.97$) and 5% ($\mu = 0.95$) of the "present day" value. The "width" of the attractive basin of equilibrium $\bar{T}^3$ appears to depend strongly on the relative intensity μ of solar insolation. For $\mu = 0.97$ this basin vanishes, $\bar{T}^{2,3}$ being a double solution of Sellers' model and for $\mu < 0.97$, $\bar{T}^1$ remains the only equilibrium. As our steady state one-dimensional climate system appears to be an analogy of the time-dependent globally integrated version (see section 2), this structural instability occurring at $\mu = 0.97$ coincides with Fraedrich's [3] analysis of a zero-dimensional energy balance model.

4. Conclusion

Some of the results described above have been derived by Ghil [6] after quite a complex mathematical analysis of Sellers' [8] model. Realizing Ghil's assumption of symmetric hemispheres (which also explains some minor quantitative differences), his figures (2a) and (6) can now be interpreted in the light of our results by showing an analogy between steady state one-dimensional and time-dependent zero-dimensional energy balance models. In this sense, our note describes an approach which gives further insight into the global stability of Sellers' one-dimensional climate model (as analysed by Ghil [6]) and which is linked with the structural analysis of a zero-dimensional climate system [3, 4].

Appendix

a) *Definition of indices in the steady state one dimensional model*

The globe is divided in 18 latitude belts, each of them 10 ° wide. The separating latitude circles (poles included) are numbered from north to south (i = 1, . . , 19). Each latitude belt has the same index as its northern boundary. The index of a latitude dependent quantity corresponds with that of the belt or circle the quantity is defined on (see appendix b; further details in [2]).

b) *Parameterization of net radiation and energy fluxes*

Net radiation and flux of total energy (see 2.2) are parameterized in the following way. For further details and values of the different constants see [2] and [8].

$$R_i = Q_i \cdot (1 - \alpha_i) - I_i \qquad \text{(B 1)}$$

where

$$\alpha_i = \begin{cases} b_i - d \cdot (T_i - \gamma Z_i) & \text{if } T_i - \gamma Z_i < 283.16\text{K} \\ b_i - d \cdot 283.16\text{K} & \text{if } T_i - \gamma Z_i \geq 283.16\text{K} \\ 0.85 & \text{if } b_i - d \cdot (T_i - \gamma Z_i) > 0.85 \end{cases}$$

$$I_i = \sigma T_i^4 \left[1 - m \cdot \tanh \left(T_i^6 \cdot 19{\cdot}10^{-16}\right)\right]$$

The meridional flux of total energy has three components: the fluxes of sensible and latent heat within the atmosphere (C_{i+1} and Lc_{i+1}) and of sensible heat in the ocean (S_{i+1}), each of which is parameterized separately.

$$C_{i+1} = \frac{c_p}{g} (\Delta)_{i+1} \cdot \left[V_{i+1} \cdot T_i - \frac{1}{\Delta y} \cdot K_{i+1}^{H} \cdot \Delta T_{i+1}\right] \qquad \text{(B 2)}$$

$$LC_{i+1} = L\,(\Delta p)_{i+1} \cdot \left[V_{i+1} \cdot \varrho_i - \frac{1}{\Delta y} \cdot K_{i+1}^{w} \cdot (\Delta q))_{i+1}\right] \qquad \text{(B 3)}$$

$$S_{i+1} = -\frac{1}{\Delta y} \cdot C_w \cdot \varrho_w \cdot (\Delta z)_{i+1} \cdot (l'/l)_{i+1} \cdot K_{i+1}^{o} \cdot (\Delta T)_{i+1} \qquad \text{(B 4)}$$

where

$$v_{i+1} = -\,a_{i+1} \cdot \left[(\Delta T)_{i+1} \pm |\overline{\Delta T}|\right] \quad \begin{matrix} i \leq 8 \\ i > 8 \end{matrix}$$

$$q_{i+1} = \frac{\varepsilon}{p} \cdot e_{i+1}$$

$$(\Delta q)_{i+1} = \frac{\varepsilon}{p} \cdot \varepsilon L/(R_l T_i^2) \cdot e_{i+1} \cdot (\Delta T)_{i+1}$$

$$e_{i+1} = \overline{e_i} \cdot \left[1 - 0.5\, \varepsilon L/(R_l T_i^2) \cdot (\Delta T)_{i+1}\right]$$

$$\overline{e_i} = \lambda \cdot 10^{\,\mu(T_i - T^*)/(\nu + T_i - T^*)}$$

$$(\Delta T)_{i+1} = T_i - T_{i+1}$$

List of symbols:

I) Constants

c_p, c_w	heat capacity of air at constant pressure and of water
d	albedo coefficient
g	acceleration of gravity
L	evaporation enthalpy of water
m	atmospheric attenuation coefficient
p	mean sea level air pressure
R_l	gas constant of dry air
$\overline{\lvert\Delta T\rvert}$	constant temperature difference for parameterization of meridional transport velocity (see [2])
Δy	width of latitude belt
γ	adiabatic lapse rate
ε	gas constant ratio of air and water vapor
λ, μ, ν, T^*	coefficients of Magnus' formula
ϱ_w	density of water
σ	Stefan-Boltzmann constant

II) Quantities defined on latitude circles

a	meridional exchange coefficient
c, C, S, F	fluxes of water vapor, sensible heat in the atmosphere and in the ocean, total energy respectively
e	saturation vapor pressure
K^w, K^H, K^o	eddy diffusivities of latent heat, sensible heat in atmosphere and ocean respectively
l, l'/l	length of latitude circle, ocean covered portion of l
Δp, Δz	pressure depth of troposphere, ocean depth
ΔT	temperature difference between adjacent latitude belts
v	meridional transport velocity

III) Quantities defined within latitude belts

A, Z	area and mean surface elevation of latitude belt
b	albedo coefficient
$\overline{e}$	saturation vapor pressure
I, Q, R	longwave emission, insolation, net radiation
T	sea level temperature
α	planetary albedo

Acknowledgments

The authors are indebted to Professor K. Fraedrich for many stimulating discussions; to Mrs. U. Eckertz-Popp and Mrs. M. Scholz for preparing the manuscript.

References

[1] Crafoord, C., Källén, E.: A note on the condition for existence of more than one steady-state solution in Budyko-Sellers type models. — J. Atmos. Sci., **35**, 1123—1125 (1978).

[2] Dümmel, Th., Volkert, H.: Eine Projektstudie über Sellers' eindimensionales, stationäres Klimamodell. — Beilage zur Berliner Wetterkarte 75/78, 15 pp (1978).

[3] Fraedrich, K.: Structural and stochastic analysis of a zero-dimensional climate system. — Quart. J. R. Met. Soc., **104**, 461—474 (1978).

[4] Fraedrich, K.: Catastrophes and resilience of a zero-dimensional climate system with ice-albedo and greenhouse effect. — Quart. J. R. Met. Soc., **105**, 147—167 (1979).
[5] Gal-Chen,T., Schneider, S. H.: Energy balance climate modelling: comparison of radiative and dynamic feedback mechanisms. — Tellus, **28**, 108—121 (1976).
[6] Ghil, M.: Climate stability for a Sellers type model. — J. Atmos. Sci., **33**, 3—20 (1976).
[7] Schneider, S. H., Gal-Chen, T.: Numerical experiments in climate stability. — J. Geophys. Res., **78**, 6182—6194 (1973).
[8] Sellers, W. D.: A global climatic model based on the energy balance of the earth-atmosphere system. — J. Appl. Meteor., 392—400 (1969).

Th. Dümmel
H. Volkert
Institut f. Meteorol.
Podbielskiallee 62
1000 Berlin 33

Eingereicht: 7. 6. 1979, angenommen: 18. 7. 1979

Meteorol. Rdsch. 33, 16–30 (Februar 1980)

Kontinent-Karten der potentiellen Landverdunstung
Mittlere Jahressummen, berechnet mit dem Penman-Ansatz

I. Henning, Münster, und

D. Henning, Bonn

Continent charts of the annual mean values of potential evapotranspiration based on Penman-concept calculations

Zusammenfassung. Unter potentieller Landverdunstung (PLV) wird die potentielle Verdunstung der realen Landoberfläche verstanden. Der Energieterm des Penman-Ansatzes wurde nach Albrecht berechnet, wobei versucht wurde, das Reflexionsvermögen der wirklichen Oberfläche mit seinen räumlichen und jahreszeitlichen Änderungen zu simulieren. Als Gebiet mit den höchsten Jahressummen tritt das nordhemisphärische Afrika hervor, wo die potentielle Landverdunstung großflächig 1700 mm/Jahr übersteigt. In den Gebirgen und Polargebieten geht die potentielle Landverdunstung mit dem Auftreten von Schnee oder Eis in extremen Lagen bis auf wenige Millimeter pro Jahr zurück.

Summary. In contrast to Penman and others, this investigation deals with the potential evapotranspiration of the real land surface. The energy term of the Penman equation was calculated after Albrecht and the albedo of the actual surface was approximated in a time- and space-dependent way. The charts reveal that the annual amounts of potential evapotranspiration are highest in Africa north of the equator exceeding 1700 mm over broad areas. The reduction of potential evapotranspiration owing to snow or ice is striking especially in mountainous and polar regions, under extreme conditions potential evapotranspiration declines to a few millimeters per year.

1. Einführung

Seit Beginn dieses Jahrhunderts ist der potentiellen Landverdunstung zunehmend Beachtung geschenkt worden, nicht zuletzt deshalb, weil diese eine der Basisgrößen der Agrarmeteorologie darstellt. Ihre direkte Messung ist problematisch; man war daher von Anfang an bemüht, sie aus verschiedenen meteorologischen Größen näherungsweise zu berechnen. Zufriedenstellende Ergebnisse wurden jedoch erst erzielt, als man die Bedeutung der Verknüpfung von Wärme- und Wasserhaushalt der Oberfläche voll erkannte und sich zugleich zutraute, die Strahlungsflüsse an der Oberfläche und damit direkt stets nur selektiv gemessene Netto-Strahlung mit für die hydro- und agrarmeteorologischen Belange hinreichender Genauigkeit zu approximieren. Damit fand das von Penman [21], [22], [23] vorgestellte, später etwas verallgemeinerte Verfahren (s. Kap. 2) erdweite Anwendung. Eine zur Zeit ihm bestehende globale Übersichtsdarstellung wurde 1970 von Chang und Okimoto [9] für die Landflächen gegeben. Die von uns vorgelegten Karten können als Ergebnisse einer Weiterführung der Untersuchung von Chang und Okimoto angesehen werden. Zur erweiterten Bearbeitung motiviert führen wir uns insbesondere durch eine veränderte Zielsetzung (s. Kap. 2); darüber hinaus meinen wir, an mehreren

0026–1211/80/0003–0016 $ 05.80